Journal of Hazardous Materials 189 (2011) 495–501

Contents lists available at ScienceDirect

Journal of Hazardous Materials

journal homepage: www.elsevier.com/locate/jhazmat

Isotherm and kinetic behavior of adsorption of anion polyacrylamide (APAM) from aqueous solution using two kinds of PVDF UF membranes

X.S. Yi[a], W.X. Shi[a], S.L. Yu[a,b,*], Y. Wang[a], N. Sun[a,c], L.M. Jin[a], S. Wang[a]

[a] State Key Laboratory of Urban Water Resource and Environment, Harbin Institute of Technology, Harbin 150090, China
[b] State Key Laboratory of Pollution Control and Resources Reuse, Tongji University, Shanghai 200092, China
[c] School of Water Conservancy & Architecture, Northeast Agricultural University, Harbin 150030, China

ARTICLE INFO

Article history:
Received 28 September 2010
Received in revised form
21 December 2010
Accepted 19 February 2011
Available online 26 February 2011

Keywords:
Adsorption
Isotherm
Kinetic
Thermodynamic parameters
UF membranes

ABSTRACT

To determine the isotherm parameters and kinetic parameters of adsorption of anion polyacrylamide (APAM) from aqueous solution on PVDF ultrafiltration membrane (PM) and modified PVDF ultrafiltration membrane (MPM) is important in understanding the adsorption mechanism of ultrafiltration processes. Effect of variables including adsorption time, initial solution concentration, and temperature were investigated. The Redlich–Peterson equation of the five different isotherm models we chose was the most fitted model, and the R^2 was 0.9487, 0.9765 for PM and MPM, respectively; while, the pseudo-first-order model was the best choice among all the four kinetic models to describe the adsorption behavior of APAM onto membranes, suggesting that the adsorption mechanism was a chemical and physical combined adsorption on heterogeneous surface. The thermodynamic parameters were also calculated from the temperature dependence ($\Delta_r G_m^\theta$, $\Delta_r H_m^\theta$, $\Delta_r S_m^\theta$), which showed that the process of adsorption is not spontaneous but endothermic process and high temperature favors the adsorption.

1. Introduction

More and more synthetic big molecular weight polyacrylamides are used in the oil field industry to enhance oil recovery in recent years [1]. Moreover, they were widely used in other industrial products and processes, such as paints, coatings, ceramics, pesticides, pharmaceuticals, cosmetics, cement, and drilling fluids [2–4]. At the same time, significant quantities of wastewater containing polyacrylamides appears, such wastewater must be treated before releasing into the environment, otherwise, its high organic content may severely pollute estuaries, rivers, lakes, soil, and even the air [5,6].

Membrane technology is widely used to treat many wastewaters, including those containing polyacrylamides, such as oil field wastewater, however, membrane fouling is ubiquitous in pressure driven membrane processes, and it would not be avoided. Membrane fouling with flux decline is caused by organic pollutants in wastewaters adsorbing irreversibly or reversibly onto the surface or within the pores of the membrane [7,8]. The seriousness of the fouling increases with operation time, leading to a serious impact on the efficiency and economics of the polyacrylamides removal process. Based on this, more and more studies on determining the mechanisms that control fouling appeared. Some studies on fouling by proteins of polymeric and PEG (polyethyleneglycol) [9,10] have been reported in the literature, however, the studies on fouling by polyacrylamides are seldom.

Increasing the hydrophilicity of membrane is a good way to reduce membrane fouling, various techniques such as chemically or radiation induced grafting and plasma polymerization have been explored for the modification of ultrafiltration membrane [11,12]. However, these methods suffer the drawbacks that inner surface of membrane cannot be modified [13]. In this study, ultrafiltration plate membrane made of PVDF (PM) and PVDF modified by TiO_2/Al_2O_3 nano-particles (MPM) through the phase-inversion method in our laboratory [14] were used. The obtained MPM will be homogeneously modified at both external and internal surfaces, and the hydrophilic property of the additive will endow the membrane with a higher hydrophilicity [15]. In general, the more hydrophilic of the membrane, the more antifouling character it will be [16,11]. However, the character of polyacrylamides is hydrophilic, which is different from most of other organic pollutants, so it is necessary to study the adsorption fouling mechanism of PM and MPM by anion polyacrylamide (APAM).

The primary focus of this paper is on understanding the effects of solution chemistry on the rate and extent of adsorption, determining the rate-limiting mechanism for adsorption onto a membrane surface, and developing a means of quantifying the fouling potential

* Corresponding author at: State Key Laboratory of Urban Water Resource and Environment, Harbin Institute of Technology, Harbin 150090, China.
Fax: +86 0454 86284101.
E-mail addresses: cedar401@163.com (X.S. Yi), hityushuili@163.com (S.L. Yu).

0304-3894/$ – see front matter © 2011 Elsevier B.V. All rights reserved.
doi:10.1016/j.jhazmat.2011.02.063

Table 1
Membrane characteristics.

Property	PVDF membrane (PM)	Modified PVDF membrane (MPM)
Skin thickness	100 nm	100 nm
Material	Polyvinylidene fluoride	Polyvinylidene fluoride-TiO_2/Al_2O_3
Pore diameter	3–5 nm	3–5 nm
MWCO	100,000 Da	100,000 Da
Hydrophobic/hydrophilic	Hydrophobic	Hydrophilic property increased

of APAM based on adsorption behavior. The adsorption isotherms and kinetics of adsorption experiments with APAM (6880 kDa) on PM and MPM membranes were performed to determine equilibrium adsorption behavior. Five adsorption models of isotherm and four models of kinetics were used to evaluate the rate-limiting processes for adsorption onto the membrane surface. Mathematical fits of these equations to experimental data allowed for the preferred models describing adsorption behavior at different solution conditions. Moreover, the kinetic and thermodynamic parameters such as standard Gibbs free energy ($\Delta_r G_m^\theta$), standard enthalpy ($\Delta_r H_m^\theta$), standard entropy ($\Delta_r S_m^\theta$), and so on were calculated to determine rate constants and analyze adsorption mechanism.

2. Materials and methods

2.1. Membranes

Ultrafiltration plate membranes used in the static adsorption experiments, were made of PVDF (or PVDF with TiO_2/Al_2O_3 nano-particles) by the phase-inversion method in our laboratory. Characteristics of membranes are shown in Table 1. All plate membranes were cut into 50 mm × 50 mm with a geometric (both side of a flat surface) area of 50 cm^2. All the new membranes were soaked in distilled water for 1 h prior to each run and used only once [16]. All the membranes were stored at 4 °C.

2.2. APAM solutions

2.2.1. Characteristics of APAM

APAM (6880 kDa) is a hydrophilic compound with a very high solubility in water, a very low isoelectric point (pH 1.8), a low octanol–water partitioning coefficient, and amide groups [4] indicating APAM would easily adsorb onto hydrophilic surfaces.

2.2.2. Preparation of APAM

The APAM stock solution was prepared by slowly adding 2.00 g APAM solid (dry weight) to 1000 ml distilled water while the solution was being stirred. The stock solution was mixed overnight before use and was therefore no less than 1 day old [17].

2.3. Adsorption experiments

Adsorption studies were performed using batch method. These experiments were conducted in 500 ml glass Erlenmeyer flasks shaken at constant temperature and 200 rpm in an air bath shaker. A volume of 300 ml of specific APAM solution was added into the flask, and then a piece of membrane with a surface area 50 cm^2, determined to be adequately sensitive for adsorption kinetics experiments was put into the solution [17]. The APAM concentration in the liquid solution was monitored at regular time intervals until equilibrium was achieved, thus obtaining the corresponding isotherm and kinetic curves. A control sample without membrane was provided for each sample accordingly. The adsorption amount was calculated based on the concentration difference of APAM in samples and control samples. Two repeats were conducted to get an average value for each sample.

2.4. Adsorption isotherm models

In order to establish the relationship between the absorption amount of APAM and corresponding equilibrium concentration in the aqueous solution, five isotherm equations most commonly used, namely Freudlich, Langmuir, Temkin, Redlich–Peterson, and Langmuir–Freundlich [18–20], have been adopted in this work. The expressions of these isotherms are presented as the following, where q is the amount adsorbed at equilibrium (μg/cm^2), C is the equilibrium concentration in solution (mg/L), and the other parameters are explained following each equation.

$$\text{Freundlich equation}: q = KC^{1/n} \quad (1)$$

where K and n are the Freundlich constants that point to relative capacity and adsorption intensity, respectively. The Freundlich model is fit for that there are many types of sites acting simultaneously, each with a different standard Gibbs free energy of adsorption, and that there is a large amount of available sites.

$$\text{Langmuir equation}: q = \frac{bq_mC}{1+bC} \quad (2)$$

where b is related to the energy of adsorption. This model is suitable for those cannot be explained clearly by Freundlich equation, such as there is a limited number of adsorption sites with the same energy that can be saturated.

$$\text{Temkin equation}: q = A + B\ln C \quad (3)$$

where A and B are Temkin constants, which reveal adsorption on the surface with per unit bounding energy; This model assumes that adsorption is characterized by a uniform distribution of binding energies [21].

$$\text{Redlich–Peterson equation}: q = \frac{aC}{1+bCn} \quad (4)$$

where a and b are the Redlich constants. This model is often used to describe chemical and physical adsorption on heterogeneous surface, instead of assumption homogeneity such as equally available adsorption sites, monolayer surface coverage, and no interaction between adsorbed species.

$$\text{Langmuir–Freundlich equation}: q = \frac{bq_mC^{1/n}}{1+bC^{1/n}} \quad (5)$$

where b and n are the Langmuir and Freundlich constants, separately. This model is used to depict that when covering a wide range of concentrations, the sorption behavior can be described neither by a linear equation nor by the Langmuir and Freundlich models [21]. In these cases, it may be necessary to apply combinations of those equations.

2.5. Calculation of thermodynamic parameters

In order to estimate the changes in the standard Gibbs free energy ($\Delta_r G_m^\theta$), standard enthalpy ($\Delta_r H_m^\theta$), and standard entropy ($\Delta_r S_m^\theta$) associated to the adsorption process, the following equations was used.

$\Delta_r G_m^\theta$ (kJ/mol) for each temperature was evaluated by

$$\Delta_r G_m^\theta = -RT\ln K \quad (6)$$

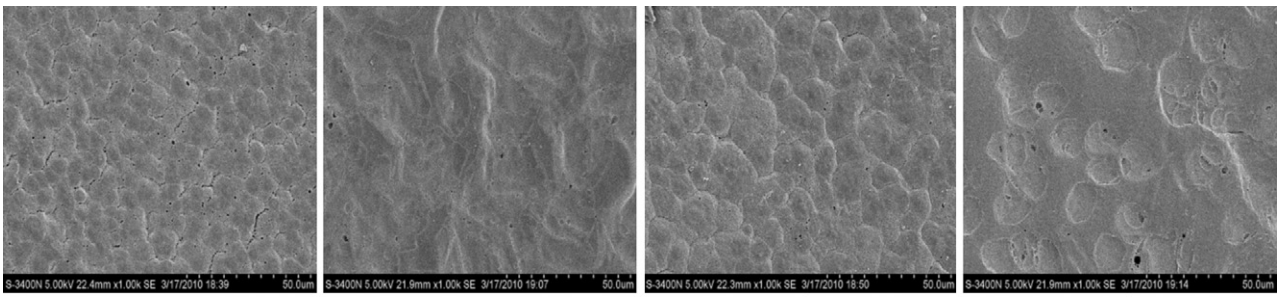

Fig. 1. SEM photographs of original PM (a), MPM (b) surface and the surface of PM (a′), MPM (b′) after adsorption of APAM.

$\Delta_r H_m^\theta$ and $\Delta_r S_m^\theta$ were determined by the Van't Hoff equation [22]:

$$\Delta_r G_m^\theta = \Delta_r H_m^\theta - T\Delta_r S_m^\theta \quad (7)$$

$$\ln K = \frac{\Delta_r S_m^\theta}{R} - \frac{\Delta_r H_m^\theta}{RT} \quad (8)$$

where the values of $\Delta_r S_m^\theta$ (J/mol K) and $\Delta_r H_m^\theta$ (kJ/mol) were obtained from the slope and intercept of the plot $\ln K$ versus $1/T$, respectively.

2.6. Adsorption kinetic models

The models of adsorption kinetics were correlated with the solution uptake rate, hence these models are important in water treatment process design [23]. In order to elucidate the adsorption mechanism and adsorption rate controlling step, four kinetic models: the pseudo-first-order equation, the pseudo-second-order equation, Elovich equation, and intra-particle diffusion equation [24–27] are tested to fit experimental data obtained from batch experiments.

$$\text{pseudo-first-order kinetic equation}: q_t = a(1 - \exp(-bt)) \quad (9)$$

where q_t (mg/cm^2) is the amount of adsorption at any time t, which has the same meanings in other equations.

$$\text{pseudo-second-order equation}: q_t = \frac{t}{1/h + t/q_e} \quad (10)$$

where h is the initial adsorption rate (μg/cm^2 h); q_e is the equilibrium adsorption capacity(μg/cm^2).

$$\text{Elovich equation}: q_t = \frac{\ln(\alpha\beta) + \ln t}{\beta} \quad (11)$$

where α is the initial adsorption rate (μg/cm^2 h), β is related to the extent of surface coverage and activation energy for chemisorption (μg/cm^2).

$$\text{intra-particle diffusion equation}: q_t = K_t t^{1/2} + C \quad (12)$$

where K_t is the intra-particle diffusion rate constant (μg/cm^2 h$^{1/2}$), C is the intercept.

3. Results and discussion

3.1. SEM of membranes surface adsorption

Fig. 1 shows the scanning electron microscope images (with a magnification of 1000) of surface characteristics difference of two kinds of membrane (PM and MPM) before and after adsorption in APAM solution for 12 h.

It can be seen from Fig. 1a and b that there is a uniform distribution of small holes and merging of small spherical particles on the original surfaces of PM and MPM, except bulge and sag on MPM is more obviously, indicating the basic morphology of membrane surface did not change after adding TiO_2 and Al_2O_3 nano-particles. Fig. 1a′ and b′ present the two membrane surfaces after adsorption of APAM. It was observed that the bulge and sag were covered by a layer of mucus-like substances which is APAM, moreover, it can be seen that the status of APAM on the surface of PM was looser compared with that on MPM, apparently. Based on this morphology, a preliminary conclusion was drawn that enhancement in adsorption capacity for MPM was attributed to the lower negative surface charge on the modified surface, and this phenomenon is similar with several reports [23,28]; furthermore, the increment of surface area may also be assumed to play a role in increasing the adsorption capacity.

3.2. Adsorption equilibrium isotherm of APAM on membranes

The results of the APAM adsorption isotherm on the two membranes experiments were shown in Fig. 2. The experimental data can be characterized by the typical L curve isotherm [29], in which the initial slope changes significantly with the solution concentration, then gently. This result was consistent with Chiem et al. who investigated polyacrylamide adsorption at the talc surface [30]. The adsorption capacity of APAM on PM and MPM membranes considerably increased with the APAM equilibrium concentration in solution, which is increasing from 0 to 9.6 μg/cm^2 and 12.6 μg/cm^2, respectively. After this, with a further increase of initial APAM concentration, the adsorption amount no longer increases significantly.

Moreover, MPM had a higher adsorption capacity than that of PM according to the results of the APAM adsorption isotherm experiments. Firstly, this may be attribute to large molecular weight and complex chemical structure of APAM. Secondly, it was believed that the surface structure changes of the material played an important role [24] in the adsorption capacity of APAM. This result was similar with adsorption of a protein (BSA) and humic acid onto a regenerated cellulose ultrafiltration membrane which was studied by Jones and O'Melia [16]. Carić et al. also indicated that membrane material and sizes of the membrane pores have a considerable influence on the amount of protein adsorbed [9]. When the PM was modified by TiO_2 and Al_2O_3 nano-particles, the surface structure was changed and the surface energy improved [14]. This led to the increasing of hydrophilicity of MPM surface, which would be significantly in favor of the adsorption of APAM. Furthermore, the surface area of MPM increased, which resulted from opening of channels and enlargement of aperture diameter and the creation of micro porosity of the material as compared with the PM also made its adsorption capacity increasing.

In general, the two-parameter equations (Langmuir, Freundlich and Temkin) are more widely used than the other three-parameter equations (Redlich–Peterson and Langmuir–Freundlich) due to the convenience of evaluating two isotherm parameters. Thus, Nakamura et al. [31] and Bowen et al. [32] were all using Langmuir

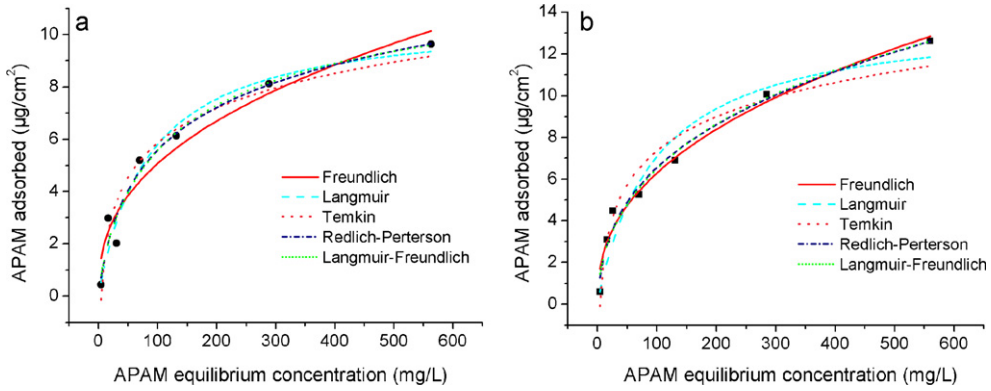

Fig. 2. APAM adsorption isotherm on PM (a) and MPM (b). Initial APAM concentration: 20 mg/L; pH 6.8; temperature: 303 K; membrane: 50 cm^2; contact time: 24 h.

equation to study the static adsorption of BSA on different membranes. However, three-parameter equations can often provide a better fit of the isotherm data than two-parameter ones.

In this paper, the experimental data of APAM adsorption on two kinds of membranes which were fitted to the five models above by non-linear regression are shown in Fig. 2, using the method of least squares. The estimated model parameters and the correlation coefficient (R^2) by origin software for the five models are shown in Table 2. It is shown that the experimental data of APAM adsorption on the two different membranes can be well fitted by these models. Clearly, the three-parameter models (Eqs. (4) and (5)) provide better fitting in R^2 values: 0.9487, 0.9487; 0.9765, 0.9720 for PM and MPM separately. The applicability order of the two-parameter isotherm models for the experimental data approximately follows: Freundlich > Langmuir ≈ Temkin. Based on this, a preliminary conclusion was drawn that the process was a chemical and physical combined adsorption on heterogeneous surface.

3.3. Thermodynamic parameters of adsorption

To determine whether the ongoing adsorption process was endothermic or exothermic in nature, APAM adsorption studies were carried out at 293 K, 298 K, 303 K, 308 K, 313 K with a constant initial APAM concentration of 20 mg/L, pH 6.8, adsorbent dose of 50 cm^2 and contact time of 12 h. The adsorption capacities of these two kinds of membranes increased with temperature increasing. Fig. 3 indicates that the process was endothermic in both cases. Meanwhile, thermodynamic parameters were calculated in Table 3.

In thermodynamics equation, the change of standard Gibbs free energy was calculated by Eq. (6), the change of entropy and heat of adsorption were calculated and estimated by Eqs. (7) and (8). Once the equilibrium constants (K) for an adsorption reaction at different temperatures are known, the standard enthalpy changes

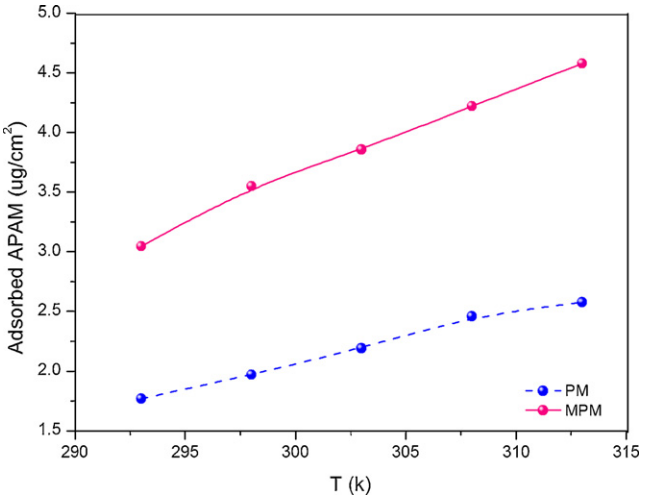

Fig. 3. Effect of temperature on APAM adsorption onto PM and MPM. Initial APAM concentration: 20 mg/L; pH 6.8; temperature: 293–313 K; membrane: 50 cm^2; contact time: 24 h.

can be calculated from the slope of a linear plot of ln K versus $1/T$ in Fig. 4, then the standard enthalpy, and standard entropy are determined.

The standard Gibbs free energy ($\Delta_r G_m^\theta$) of APAM adsorption on PM was 5.68, 5.48, 5.27, 5.03, and 4.97 kJ/mol at 293, 298, 303, 308, and 313 K, respectively, while on MPM was 4.18, 3.80, 3.61, 3.37, 3.16 kJ/mol, accordingly. The standard Gibbs free energy of the process at all temperatures for APAM adsorption onto the two membranes was positive, indicating that it is hard for APAM adsorbed by PM and MPM; namely, the feasibility of this adsorption process is non-spontaneous. The positive value decreased with

Table 2
Estimated isotherm parameters for APAM adsorption on PM and MPM membranes.

Freundlich equation $q = KC^{1/n}$	Parameter	k	$1/n$		R^2
	PM	0.8026	0.4005		0.9382
	MPM	0.9352	0.4141		0.9643
Langmuir equation $q = bq_mC/(1+bC)$	Parameter	q_m	B		R^2
	PM	10.7732	0.0117		0.9323
	MPM	13.8737	0.0104		0.9339
Temkin equation $q = A + B\ln C$	Parameter	A	B		R^2
	PM	−2.9523	1.914		0.9367
	MPM	−3.4960	2.357		0.9428
Redlich–Peterson equation $q = aC/(1+bCn)$	Parameter	a	b	n	R^2
	PM	0.1889	0.0514	0.8326	0.9487
	MPM	0.5993	0.3793	0.6658	0.9765
Langmuir–Freundlich $q = bq_mC^{1/n}/(1+bC^{1/n})$	Parameter	q_m	b	$1/n$	R^2
	PM	12.8314	0.0213	0.779	0.9487
	MPM	35.1328	0.0202	0.5251	0.9720

Table 3
Thermodynamic parameters of APAM adsorption onto PM and MPAM membranes.

APAM-membranes system	$\Delta_r G_m^\theta$ (KJ/mol)					$\Delta_r H_m^\theta$ (KJ/mol)	$\Delta_r S_m^\theta$ (J/mol K)
	293 K	298 K	303 K	308 K	313 K		
PM membrane	5.68	5.48	5.27	5.03	4.97	18.632	49.529
MPM membrane	4.18	3.80	3.61	3.37	3.16	16.690	37.625

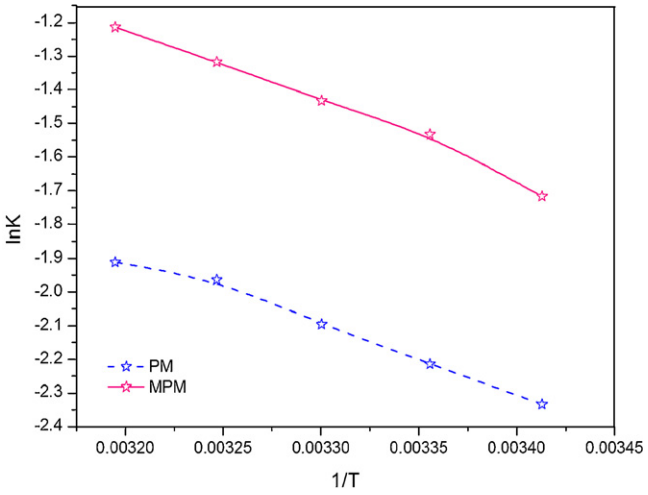

Fig. 4. Van't Hoff plots of APAM adsorption onto PM and MPM for different temperature. Initial APAM concentration: 20 mg/L; pH 6.8; temperature: 293–313 K; membrane: 50 cm^2; contact time: 24 h.

temperature increasing, suggesting that the possibility of adsorption is proportional to the temperature. Moreover, positive values of $\Delta_r H_m^\theta$ indicate the endothermic nature of the process. Obviously, the results in Table 3 show that temperature has a positive affection on the adsorption process of the APAM, because higher temperatures provide more energy to enhance the adsorption rate. Moreover, the standard enthalpy change of adsorption of APAM by PM and MPM were 18.632 and 16.690 kJ/mol separately. Alkan pointed out that when the standard enthalpy change between 40 and 120 kJ/mol, the adsorption is chemisorption, otherwise the adsorption is physicosorption [27]. Therefore, this adsorption process seems to be physisorption. The standard entropy change ($\Delta_r S_m^\theta$) of APAM adsorbed by PM and MPM were 49.529, 37.625 J/mol K, respectively, reflects that the distribution of APAM adsorbed by the two membranes was more chaotic than that in the aqueous solution, this changes for the process could be due to a combination of the affinity of the membranes with APAM in solvent dissociation events.

3.4. Kinetics of adsorption of APAM on membranes

As has been shown that the adsorption capacities of these two membranes for APAM were high, thus, it is necessary to study the kinetic models of this adsorption process. The kinetic experiments were performed at the initial pH 6.8 and temperature 30 °C. The reason we chose these two parameters was that pH of oilfield raw wastewater is about 10 and temperature is about 40 °C commonly, however, after pretreatment by conventional processes such as adding acid destabilization/coagulation/sedimentation/filtration, etc., pH and temperature is often around 7.0 (6.8–7.2) and 30 °C, respectively.

3.4.1. Effect of initial concentration

In order to elucidate the effect of initial concentration, four kinetic models were tested to fit experimental data obtained from batch APAM adsorption experiments. The kinetic experiments were performed at pH 6.8 for the initial APAM concentrations of 10 mg/L, 100 mg/L and 300 mg/L under 30 °C. Four types of APAM adsorption rates were obtained by following decrease of the concentration with contact time are shown in Fig. 5. It was about 12 h to reach equilibrium for the removal of APAM from aqueous solution, after this, the amount of adsorbed APAM did not change significantly with time. The estimated parameters and kinetic equation with correlation coefficient are shown in Table 4.

Fig. 5. shows that the kinetics of adsorption of APAM by PM and MPM membranes consisted of two phases: an initial rapid phase, which was fast and contributed significant to equilibrium uptake; a slower second phase, its contribution to the total adsorption was relatively small. Moreover, the equilibrium occurs relatively earlier in the solution of low APAM concentrations than the higher ones. The necessary time to reach equilibrium is not identical according to the initial concentration, about 4 h (10 mg/L), 6 h (100 mg/L), and 10 h (300 mg/L). It also can be observed that the capacity of APAM removal both by PM and MPM membranes at equilibrium increased with the initial concentration, about 0.899 μg/cm^2, 5.60 μg/cm^2, 6.71 μg/cm^2 on PM, and 1.26 μg/cm^2, 9.60 μg/cm^2, 12.06 μg/cm^2 on MPM. This is because more efficient utilisation of the adsorption capacities of the adsorbent, which is expected due to a greater driving force by a higher concentration gradient pressure [29]. Thus,

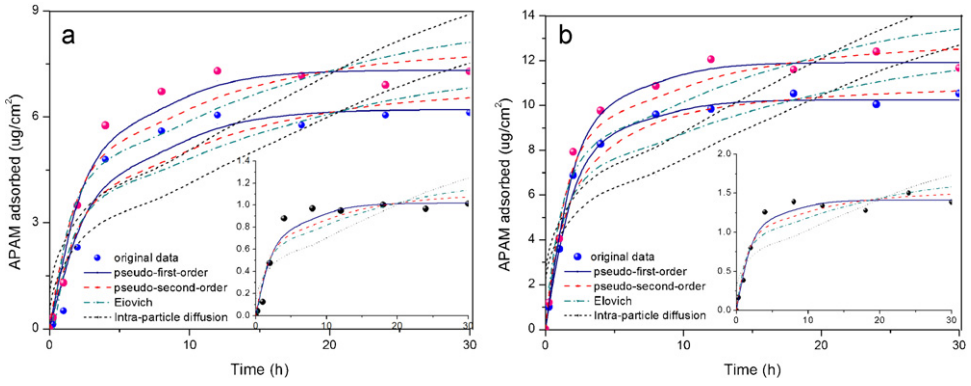

Fig. 5. Kinetics curve of APAM adsorption APAM adsorption isotherm on PM (a) and MPM (b) at 30 °C, 10 mg/L, 100 mg/L, 300 mg/L, pH 6.8, membrane: 50 cm^2; contact time: 24 h.

Table 4
Kinetic parameters for the adsorption of APAM on PM and MPM membranes.

Model/factor			Pseudo-first-order model			Pseudo-second-order model	
			a	b	R^2	$1/h$	R^2
C_0 (mg/L)	10	PM	1.0171	0.3265	0.9638	2.2405	0.9294
		MPM	1.4091	0.4112	0.9774	1.1911	0.9526
	100	PM	6.2051	0.2712	0.9614	0.4600	0.9301
		MPM	10.256	0.4385	0.9953	0.1430	0.9875
	300	PM	7.321	0.3168	0.9838	0.3133	0.9533
		MPM	11.920	0.4344	0.9956	0.1281	0.9838
T (K)	293	PM	1.7592	0.2951	0.9614	1.4080	0.9276
		MPM	3.1645	0.3689	0.9762	0.6019	0.9506
	303	PM	2.1507	0.3200	0.9604	1.0733	0.9411
		MPM	3.9405	0.4032	0.9802	0.0824	0.9552
	313	PM	2.5042	0.3363	0.9763	0.1713	0.9532
		MPM	4.6213	0.4108	0.9890	0.3454	0.9682

Model/factor			Elovich model			Intra-particle diffusion model		
			α	β	R^2	K_t	C	R^2
C_0 (mg/L)	10	PM	1.0134	4.2902	0.8894	0.2020	0.1362	0.7122
		MPM	2.2441	3.4455	0.9071	0.2635	0.2901	0.7070
	100	PM	4.9404	0.6749	0.8988	1.2758	0.5328	0.7527
		MPM	17.994	0.4801	0.9491	1.9064	2.2506	0.7350
	300	PM	7.5485	0.6064	0.9156	1.4417	1.0084	0.7402
		MPM	20.9457	0.4143	0.9475	2.2034	2.6317	0.7246
T (K)	293	PM	1.6378	2.7165	0.8696	0.2487	0.3656	0.6326
		MPM	2.2545	0.2232	0.8878	0.0927	0.3795	0.6403
	303	PM	2.2267	2.2573	0.8971	0.3065	0.4654	0.6748
		MPM	4.5624	0.2026	0.8853	0.1144	0.4687	0.6179
	313	PM	3.1136	2.0338	0.8959	0.0737	0.3020	0.6499
		MPM	10.900	1.2670	0.9005	0.5750	1.4639	0.6270

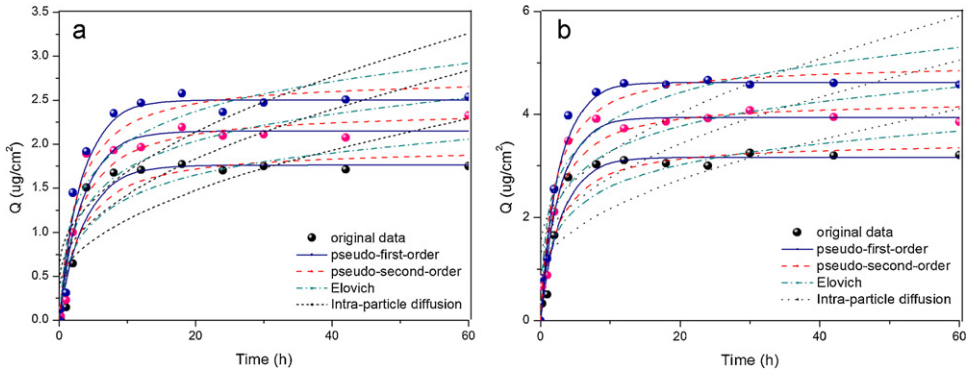

Fig. 6. Kinetics curve of APAM adsorption APAM adsorption isotherm on PM (a) and MPM (b) at 20 °C, 30 °C, 40 °C, 20 mg/L, pH 6.8, membrane: 50 cm^2; contact time: 24 h.

12 h could be chosen as equilibrium adsorption time to make sure that equilibrium was reached.

3.4.2. *Effect of temperature*

A large number of oil field effluents are produced at a relatively high temperature, therefore, temperature can be an important factor for the UF process. Fig. 6 shows the four kinetic models were used to fit experimental data obtained from the kinetic experiments, which were performed at pH 6.8 with APAM concentration of 20 mg/L, under 293 K, 313 K, 323 K. The estimated parameters and R^2 value are shown in Table 4.

Fig. 6 provides the results of APAM adsorption kinetic experiments on two different membranes at 293 K, 313 K and 323 K. It can be seen that the adsorption rate was slightly higher at a higher temperature. Moreover, the majority of APAM adsorption on membranes was completed in about 4 h. For example, the adsorption capacities of PM membrane for APAM were 0.228, 1.002, 1.891 mg/cm^2 after 1 h, 2 h, and 4 h at 293 K, which was about 14%, 37% and 86% of the equilibrium capacity (2.112 mg/cm^2), respectively. In this paper, the constants of APAM adsorption kinetic were fitted with four models under different initial concentrations and temperatures by non-linear regression were shown in Table 4. All of R^2 values of this adsorption process on two different membranes by pseudo-first-order kinetic model are higher than 0.96, indicating the adsorption kinetic process is following this kinetic model. This is generally in agreement with other research result that the first-order kinetic model was able to describe properly the kinetic process of dyes adsorption onto different industrial waste adsorbents [18]. Two kinetic equations were not well-described adsorption of the APAM on all the membranes, especially, the intra-particle diffusion model. This is because APAM adsorption onto membranes is dominated and controlled by the external surface adsorption or the instantaneous adsorption stage.

4. Conclusion

The adsorption behavior of APAM by PVDF membranes (PM) and modified PVDF membranes (MPM) was studied. All the selected five

isotherm models fitted the adsorption well, applicability order of two parameters model: Freundlich > Langmuir ≈ Temkin, and the Redlich–Peterson and Langmuir–Freundlich equation were more suitable, which provided better fitting with R^2 values: 0.9487, 0.9487; 0.9765, 0.9720 for PM and MPM, separately. The results of the study clearly showed that MPM has a higher adsorption capacity of APAM, and the amount of the adsorption was positively proportional to temperature (293–313 K) and initial concentration varying from 0 to 300 mg/L. Adsorption reaction reached equilibrium during 12 h of contact time, and this process was endothermic. This adsorption kinetics conformed to pseudo-first-order (PFO) model, and all R^2 values are higher than 0.96. Moreover, though the adsorption of APAM by the membranes was not spontaneous, it was easier to be adsorbed on MPM.

Acknowledgements

The authors gratefully acknowledge State Key Laboratory of Urban Water Resource and Environment, Harbin Institute of Technology, for its support during the conduct of this research. Thanks are also extended to Professor Liping Sun, Tianjin Institute of Urban Construction, China, for several insightful comments in the preparation of this paper. We also appreciate the editor and reviewers' valuable comments very much, which are helpful to improve the quality of our present study.

References

[1] X.F. Zhao, L.X. Liu, Y.C. Wang, H.X. Dai, D. Wang, H. Cai, Influences of partially hydrolyzed polyacrylamide (HPAM) residue on the flocculation behavior of oily wastewater produced from polymer flooding, Sep. Purif. Technol. 62 (2008) 199–204.
[2] D.A. Beattie, L. Huynh, G.B. Kaggwa, J. Ralston, Influence of adsorbed polysaccharides and polyacrylamides on talc flotation, Int. J. Miner. Process. 78 (2006) 238–249.
[3] Y.H. Ni, H.Y. Zhang, J.M. Hong, L. Zhang, X.W. Wei, PAM-directed fabrication, shape evolution and formation mechanism of $BaCO_3$ crystals with higher-order superstructures, J. Crystal Growth 310 (2008) 4460–4467.
[4] Q. Zhang, Y. Gao, Y.A. Zhai, F.Q. Liu, G. Gao, Synthesis of sesbania gum supported dithiocarbamate chelating resin and studies on its adsorption performance for metal ions, Carbohydr. Polym. 73 (2008) 359–363.
[5] Z. Chen, G.H. Huang, J.B. Li, A GIS-based modeling system for petroleum waste management, Water Sci. Technol. 47 (2003) 309–317.
[6] S.F.V. Jerez, J.M. Godoy, N. Miekeley, Environmental impact studies of barium and radium discharges by produced waters from the "Bacia de Campos" oil-field offshore platforms Brazil, J. Environ. Radioact. 62 (2002) 29–38.
[7] S.H. Wu, B.Z. Dong, Y. Huang, Adsorption of bisphenol A by polysulphone membrane, Desalination 253 (2010) 22–29.
[8] F. Cattoli, C. Boi, M. Sorci, G.C. Sarti, Adsorption of pure recombinant MBP-fusion proteins on amylose affinity membranes, J. Membr. Sci. 273 (2006) 2–11.
[9] M.Đ. Carić, S.D. Milanović, D.M. Krstić, M.N. Tekić, Fouling of inorganic membranes by adsorption of whey proteins, J. Membr. Sci. 165 (2000) 83–88.
[10] X.L. Ma, Y.L. Su, Q. Sun, Y.Q. Wang, Z.Y. Jiang, Preparation of protein-adsorption-resistant polyethersulfone ultrafiltration membranes through surface segregation of amphiphilic comb copolymer, J. Membr. Sci. 292 (2007) 116–124.
[11] M. Taniguchi, G. Belfort, Low protein fouling synthetic membranes by UV assisted surface grafting modification: varying monomer type, J. Membr. Sci. 231 (2004) 147–157.
[12] A.V.R. Reddy, D.J. Mohan, A. Bhattacharya, V.J. Shah, P.K. Ghosh, Surface modification of ultrafiltration membranes by preadsorption of a negatively charged polymer. I. Permeation of water soluble polymers and inorganic salt solutions and fouling resistance properties, J. Membr. Sci. 214 (2003) 211–221.
[13] L.F. Hancock, S.M. Fagan, M.S. Ziolo, Hydrophilic, semipermeable membranes fabricated with poly(ethylene oxide)-polysulfone block copolymer, Biomaterials 21 (2000) 725–733.
[14] S.L. Yu, Y. Lu, B.X. Chai, J.H. Liu, Treatment of oily wastewater by organic–inorganic composite tubular ultrafiltration (UF) membranes, Desalination 196 (2006) 76–83.
[15] J. Mueller, R.H. Davis, Protein fouling of surface-modified polymeric microfiltration membranes, J. Membr. Sci. 116 (1996) 47–60.
[16] K.L. Jones, C.R. O'Melia, Protein and humic acid adsorption onto hydrophilic membrane surfaces: effects of pH and ionic strength, J. Membr. Sci. 165 (2000) 31–46.
[17] M.L. Taylor, G.E. Morris, P.G. Self, St. Roger, C. Smart, Kinetics of adsorption of high molecular weight anionic polyacrylamide onto kaolinite: the flocculation process, J. Colloid Interface Sci. 250 (2002) 28–36.
[18] C. Do, Adsorption design for wastewater treatment, Lewis Publishers, Boca Raton, FL, USA, 1998.
[19] L. Zeng, X.M. Li, J.D. Liu, Adsorptive removal of phosphate from aqueous solutions using iron oxide tailings, Water Res. 38 (2004) 1318–1326.
[20] R.D. Johnson, F.H. Arnold, The temkin isotherm describes heterogeneous protein adsorption, Biochem. Biophys. Acta 1247 (1995) 293–297.
[21] I.X. García-Zubiri, G. González-Gaitano, J.R. Isasi, Sorption models in cyclodextrin polymers: Langmuir, Freundlich, and a dual-mode approach, J. Colloid. Interface Sci. 337 (2009) 11–18.
[22] C. Namasivayam, K. Ranganathan, Waste Fe(III)/Cr(III) hydroxide as adsorbent for the removal of Cr(VI) from aqueous solution and chromium plating industry wastewater, Environ. Pollut. 82 (1993) 255–261.
[23] W.H. Zou, R.P. Han, Z.Z. Chen, J.H. Zhang, J. Shi, Kinetic study of adsorption of Cu(II) and Pb(II) from aqueous solutions using manganese oxide coated zeolite in batch mode, Colloid Surf. A: Physicochem. Eng. Asp. 279 (2006) 238–246.
[24] Y.G. Xue, H.B. Houa, S.J. Zhua, Adsorption removal of reactive dyes from aqueous solution by modified basic oxygen furnace slag: Isotherm and kinetic study, Chem. Eng. J. 147 (2009) 272–279.
[25] Q.L. Fu, Y.L. Deng, H.S. Li, J. Liu, H.Q. Hu, S.W. Chen, Sa. Tongmin, Equilibrium, kinetic and thermodynamic studies on the adsorption of the toxins of *Bacillus thuringiensis* subsp. kurstaki by clay minerals, Appl. Surf. Sci. 255 (2009) 4551–4557.
[26] C.W. Cheung, J.F. Porter, G. Mckay, Sorption kinetics for the removal of copper and zinc from effluents using bone char, Sep. Purif. Technol. 19 (2000) 55–64.
[27] M. Alkan, O. Demirbas, S. Celikcapa, M. Dogan, Sorption of acid red 57 from aqueous solution onto sepiolite, J. Hazard. Mater. 116 (2004) 135–145.
[28] E. Allen, G. Fu, C. Cowan, Adsorption of cadimium and copper by manganese oxide, Soil Sci. 152 (1991) 72–81.
[29] C. Nathalie, G. Richard, D. Eric, Adsorption of Cu(II) and Pb(II) onto a grafted silica: isotherms and kinetic models, Water Res. 37 (2003) 3079–3086.
[30] L.T. Chiem, L. Huynh, J. Ralston, D.A. Beattie, An insitu ATR–FTIR study of polyacrylamide adsorption at the talc surface, J. Colloid Interface Sci. 297 (2006) 54–61.
[31] K. Nakamura, K. Matsumoto, Adsorption behavior of BSA in microfltrationwith porous glass membrane, J. Membr. Sci. 145 (1998) 119–128.
[32] W.R. Bowen, D.T. Hughes, Properties of microfiltration membranes. Part 2. Adsorption of bovine serum albumin at aluminum oxide membranes, J. Membr. Sci. 51 (1990) 189–200.